Black-colored ZnO nanowires with enhanced photocatalytic hydrogen evolution

2016 Nanotechnology 27 22LT01

(http://iopscience.iop.org/0957-4484/27/22/22LT01)

IOP Publishing
Letters
Nanotechnology
Nanotechnology 27 (2016) 22LT01 (6pp)
doi:10.1088/0957-4484/27/22/22LT01

Letter

Black-colored ZnO nanowires with enhanced photocatalytic hydrogen evolution

Nan Zhang[1,2], Chong-Xin Shan[1,3,7], Hua-Qiao Tan[1], Qi Zhao[3], Shuang-Peng Wang[1,4], Zai-Cheng Sun[1,5], Yong-de Xia[6] and De-Zhen Shen[1]

[1] State Key Laboratory of Luminescence and Applications, Changchun Institute of Optics, Fine Mechanics and Physics, Chinese Academy of Sciences, Changchun 130033, People's Republic of China
[2] University of Chinese Academy of Sciences, Beijing 100049, People's Republic of China
[3] School of Physics and Engineering, Zhengzhou University, 450001, People's Republic of China
[4] Institute of Applied Physics and Materials Engineering, University of Macau, Avenida da Universidade, Taipa, Macau, People's Republic of China
[5] School of Environmental and Energy Engineering, Beijing University of Technology, Beijing 100124, People's Republic of China
[6] College of Engineering, Mathematics and Physical Sciences, University of Exeter, Exeter, EX4 4QF, UK

E-mail: shancx@ciomp.ac.cn

Received 23 January 2016, revised 4 April 2016
Accepted for publication 12 April 2016
Published 25 April 2016

Abstract

Black-colored ZnO nanowires have been prepared in a metal–organic chemical vapor deposition system by employing a relatively low growth temperature and oxygen-deficient conditions. X-ray photoelectron spectroscopy reveals the incorporation of carbon into the nanowires. The photocatalytic hydrogen evolution activity of the black-colored ZnO nanowires is over 2.5 times larger than that of the pristine ZnO nanowires under simulated solar illumination conditions, and the enhanced photocatalytic activity can be attributed to the higher absorption of visible light by the black color and better carrier separation at the ZnO/carbon interface.

Keywords: photocatalysis, hydrogen evolution, ZnO, black color

(Some figures may appear in colour only in the online journal)

1. Introduction

Due to its abundance, low cost, and environmental friendliness [1–3], ZnO has been considered as a promising candidate for photocatalysis [4–7]. Many reports have demonstrated the photocatalytic activity of ZnO and related materials [8–17]. Nevertheless, the absorption of ZnO is mainly located in the ultraviolet (UV) region because of its wide bandgap (3.37 eV at room temperature). Considering that less than 5% of the solar energy exists in the UV region, a very small portion of solar energy can be utilized by ZnO-based photocatalysts, which hinders the realization of efficient photocatalysis of ZnO under solar illumination conditions. Thus, to enhance the photocatalytic activities of ZnO, utilizing the visible light more effectively is essential. Different kinds of dopants have been introduced into ZnO to increase the visible light absorbance by modifying the bandgap of ZnO [17–27]. However, the incorporation of dopants usually deteriorates the crystalline quality of ZnO, which is unfavourable to its photocatalytic activity. Color-changing is the intuitive expression of the enhanced absorption of visible light. If a material is black in color, it means that this material can absorb visible light. Black TiO_2 has been prepared by heating crystalline TiO_2 nanocrystals in a high-pressure hydrogen environment, and the black TiO_2 nanoparticles showed much higher photocatalytic activity in hydrogen evolution measurement [28–30]. Recently, black ZnO powders with enhanced visible light absorption and photocatalytic activity

[7] Author to whom any correspondence should be addressed.

have also been demonstrated by the same group [31]. Compared with the doping route, hydrogen treatment produces a thin disorder layer at the surface of the ZnO nanoparticles, which does not deteriorate the crystallinity of the ZnO core. However, a relatively complex process is usually involved in this approach: a high-pressure (20 bar), dangerous gas (hydrogen), and elevated temperature (400 °C) are necessary in the procedure, all of which hinder greatly the applicability of this approach.

In this work, black-colored ZnO nanowires have been achieved by employing a one-step metal–organic chemical vapour deposition (MOCVD) growth route under relatively low temperature and oxygen-deficient growth conditions. X-ray photoelectron spectroscopy (XPS) reveals the incorporation of carbon into the ZnO, and transmission electron microscopy (TEM) indicates the crystalline nature of the nanowires. The photocatalytic activity of the black-colored nanowires is 2.5 times higher than that of the pristine ZnO nanowires under simulated solar irradiation conditions, which can be attributed to the higher absorption of visible light and better separation of electrons and holes at the ZnO/carbon interface.

2. Experimental method

2.1. Synthetic procedures

The ZnO nanowires were prepared in a MOCVD apparatus on a sapphire substrate. Such a technique is widely used for the growth of ZnO. The precursors used for the growth were diethylzinc and oxygen, and the carrier gas that leads the precursors into the growth chamber was high-purity (9N) nitrogen. Prior to the growth, the sapphire substrates were treated at 800 °C under 10^{-4} Pa for 60 min to remove the possible adsorbed contaminants on the substrate. Then the substrate temperature was lowered to 550 °C and the flow rate of O_2 was kept at 30 sccm during the growth process. The diethylzinc and oxygen reacted incompletely in this way, thus some of the carbon in the diethylzinc was incorporated into the ZnO. Pristine ZnO nanowires, which are white in color, were also been prepared as a control sample. For the growth of the pristine ZnO sample, the temperature was kept at 700 °C and the flow rate of O_2 was kept at 60 sccm during the growth process. The chamber pressure in both cases was fixed at 3000 Pa.

2.2. Photocatalytic H_2 evolution

To test the photocatalytic activity of the pristine and black-colored ZnO nanowires, the samples were placed into a methanol solution (120 ml, 25%) in a closed gas circulation system (Perfect Light Company Labsolar-III (AG)). The simulated solar and visible light irradiation were obtained from a 300 W Xe lamp (Perfect Light Company Solaredge700) without and with a UVIRCUT filter (Newport) (400–800 nm), respectively. Methanol was used as a sacrificial reagent. The amount of generated H_2 was determined by online gas chromatography (SchimazuGC-2014c).

3. Results and discussion

3.1. Structural and optical properties

The morphology and structural characterizations of the pristine ZnO samples are shown in figure 1. One can see from figure 1(a) that nanowire-shaped structures were formed with a length of about 600 nm. The TEM image of an individual nanowire shown in the inset of figure 1(a) reveals that the diameter of the nanowire tapers from the base to the top, and the size at the base is around 30 nm, while that at the top is less than 10 nm. The high-resolution TEM image of an individual ZnO nanowire is shown in figure 1(b). Clear lattice fringes can be observed, indicating the high crystalline quality of the nanowires. The length between two adjacent lattice fringes is around 0.26 nm, which corresponds to the *d*-spacing of the (002) plane in hexagonal ZnO. From the lattice fringes, one can also see that the nanowires were grown along the [002] direction. The selected area electron diffraction (SAED) pattern of the nanowires is shown in figure 1(c), and the clear dotted pattern reveals the single crystalline nature of the nanowires. The XRD pattern of the pristine ZnO nanowires is shown in figure 1(d). Only two peaks at around 34.4°and 72.5° are visible from the pattern besides the diffraction from the sapphire substrate, which can be indexed to the diffraction from the (002) and (004) facet of wurtzite ZnO, respectively.

The morphology and structural properties of the carbon-incorporated ZnO nanowires were also evaluated by SEM, HRTEM, SAED and XRD, as shown in figures 2(a)–(d). It is observed from figure 2(a) that the nanowires also show a tapered shape with a similar size with the pristine nanowires. Like the pristine nanowires, a high-resolution TEM image shows clear lattice fringes and the SAED pattern shows clear dotted patterns, revealing the high crystalline quality of this kind of nanowire. Note that the (002) diffraction peak of the carbon-incorporated ZnO is located at 34.3°, which is slightly smaller than that of the pristine ZnO. We think the shift to a smaller angle side indicates that carbon has been alloyed into the lattice of ZnO.

The chemical states and composition of the pristine and carbon-incorporated ZnO nanowires are shown in figure 3(a). One can see that the patterns for the two samples are very similar, and all the peaks can be ascribed to O, Zn and C. The O1s peaks are located at about 530.2 eV and 531.8 eV, which can be attributed to the binding energy of O in ZnO and adsorbed oxygen, respectively. The C1s peak is located at 284.6 eV for the both samples; note that in both samples, the C1s peak has a symmetrical Gaussian shape, which means that the carbon exists in a single bonding state. In order to identify the existence of carbon in the inner part of the samples, the two samples were etched by argon ions for 5 min, and the XPS spectra of the etched samples are shown in figures 3(b) and (c). It is evidenced that, for both samples, there are strong C1s signals in the as-grown sample, but after

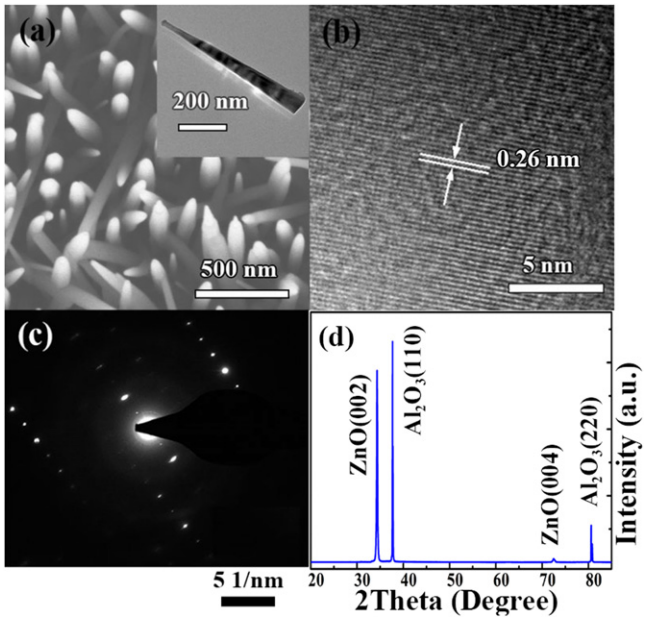

Figure 1. (a) SEM image of the pristine ZnO nanowires; the inset shows a TEM image of an individual nanowire. (b) HRTEM image, (c) SAED pattern and (d) θ–2θ XRD pattern of the pristine ZnO nanowires.

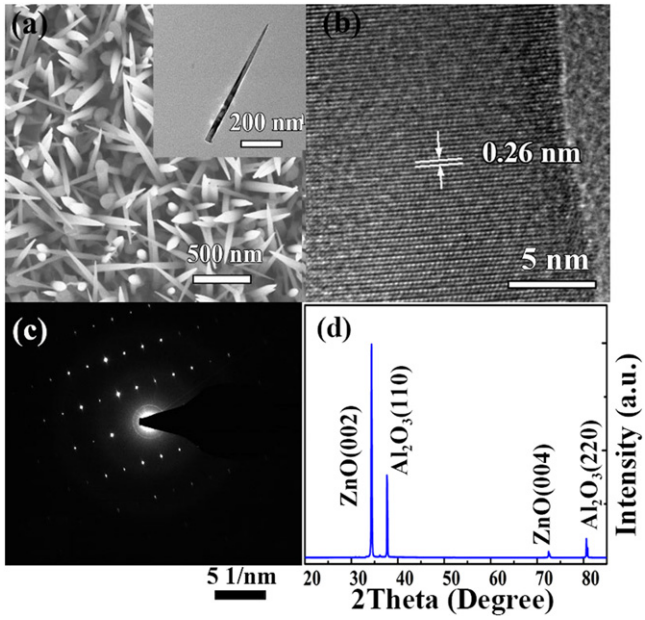

Figure 2. (a) SEM image of the carbon-incorporated ZnO nanowires; the inset shows a typical TEM image of an individual nanowire. (b) HRTEM image, (c) SAED pattern and (d) θ–2θ XRD pattern of the carbon-incorporated ZnO nanowires.

the etching process, the intensity of the C1s signal decreases greatly for the pristine ZnO nanowires, indicating that the carbon in the pristine nanowires is mainly located at the surface, and the origin of the carbon may be due to the adsorption or contamination of carbon or organics. In contrast, for the carbon-incorporated ZnO sample, the C1s signal decreases little after the etching process, and the atom ratio of

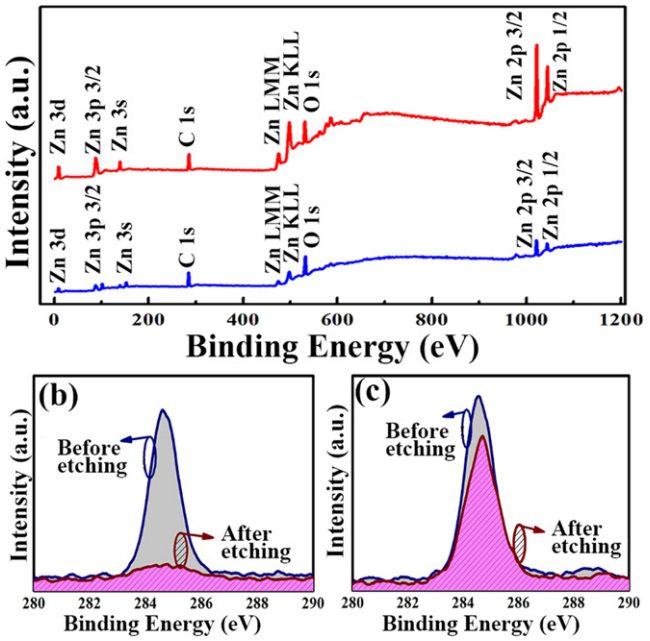

Figure 3. (a) XPS survey spectrum of the pristine and carbon-incorporated ZnO nanowires. (b) XPS spectra of C1s in the pristine ZnO before and after a 5 min etching. (c) XPS spectra of C1s in the carbon-incorporated ZnO before and after 5 min of etching.

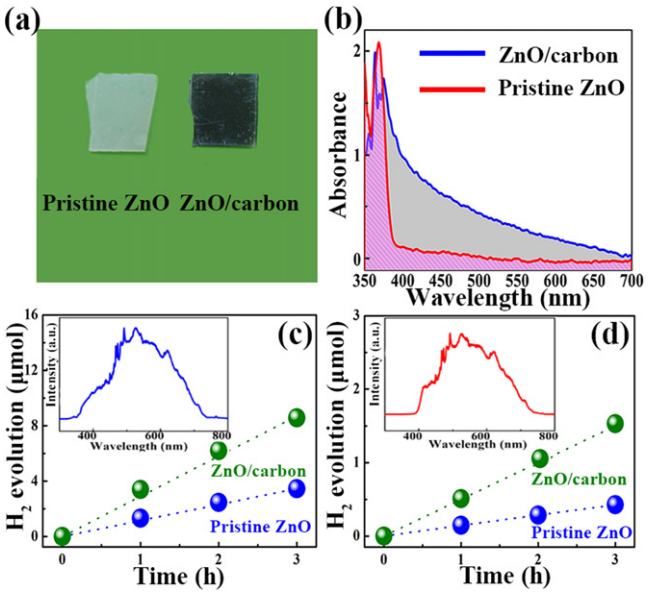

Figure 4. (a) Photograph of the pristine and carbon-incorporated ZnO sample. (b) Absorption spectra of the pristine and carbon-incorporated ZnO nanowires. (c) Photocatalytic hydrogen evolution of the pristine and carbon-incorporated ZnO nanowires under simulated solar light; the inset is the spectrum of simulated solar light (Xe lamp). (d) Irradiation-time dependence of H_2 production for the pristine and carbon-incorporated ZnO nanowires under visible light; the inset is the spectrum of visible light (Xe lamp with a 400–800 nm UVIRCUT filter). Note that the dots in (c) and (d) are experimental data, while the dotted lines are linear fitting results to the experimental data.

C1s is determined to be around 27.2% after etching, indicating that there is still much carbon in the inner part of the nanowires besides the adsorbed carbon on the sample surface.

Table 1. A list of reported hydrogen production data for ZnO-based materials under UV–visible radiation conditions.

Material	Irradiation source	Hydrogen production efficiency (μmol g^{-1} h^{-1})	Reference
Black-colored ZnO/carbon nanowires	300 W Xe lamp	1847.9	Our result
Ce-doped ZnO/ZnS	UV lamp	1200	[32]
ZnS/ZnO	One sun irradiation	494.8	[33]
CdS/Au/ZnO	—	600	[34]
MoS_2/ZnO	300 W Xe lamp	768	[35]
Hydrogenated ZnO	300 W Xe lamp	122 500	[36]

The photograph of the pristine and carbon-incorporated ZnO nanowire sample is illustrated in figure 4(a). One can see that the carbon-incorporated sample is black in color to the naked eye, which is distinctively different from the milky color of the pristine ZnO nanowires. This is the first report of black-colored ZnO obtained by the common growth method to the best of our knowledge. The absorption spectra of the pristine and carbon-incorporated ZnO nanowires are shown in figure 4(b). There is a strong absorption peak at around 370 nm for both samples, which corresponds to the near-band-edge absorption of ZnO. An obvious absorption tail can be observed in the visible region for the black-colored sample, while for the pristine sample the absorption in the visible region is much weaker. The increased absorption in the visible region may be of help in increasing the photocatalytic activity of the sample under solar illumination conditions.

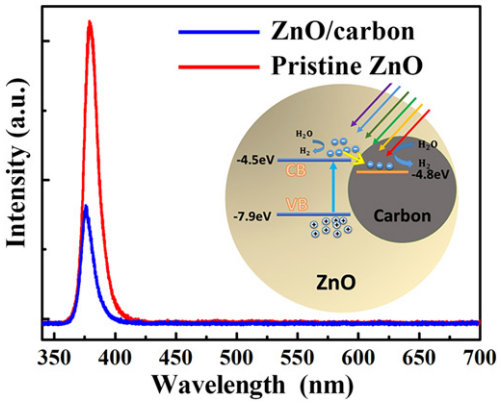

Figure 5. The PL spectra of the pristine ZnO and ZnO/carbon samples at 300 K; the inset is the schematic illustration of the carrier separation at the ZnO/carbon interface.

3.2. Photocatalytic activity

The photocatalytic activity of the carbon-incorporated black ZnO nanowires was evaluated by measuring the H_2 production under simulated solar light and visible light irradiation, the results of which are shown in figures 4(c) and (d). To measure the hydrogen evolution, pristine and carbon-incorporated samples of similar size were placed into an aqueous methanol solution (120 ml, 25%) in a closed gas circulation system. A 300 W Xe lamp was used as the light source. The carbon-incorporated sample produced 8.6 μmol H_2 in three hours (corresponding to 1847.9 μmol g^{-1} h^{-1}) under the simulated solar light, which is about 2.5 times that produced by the pristine ZnO. To access the photocatalytic activity of the carbon-incorporated ZnO nanowires under the illumination of visible light, the H_2 production data were collected under the illumination of a Xe lamp with a 400–800 nm UVIRCUT filter, as shown in figure 4(d). One can see that the carbon-incorporated sample produces 1.5 μmol H_2 in three hours (corresponding to 277.3 μmol g^{-1} h^{-1}), which is about three times that produced by the pristine ZnO sample under the same irradiation conditions. The above results mean the improved photocatalytic ability of the carbon-incorporated sample is mainly caused by the enhanced photocatalytic performance in the visible region. Table 1 presents a list of the reported hydrogen production efficiencies of ZnO-based materials under UV–visible radiation, and one can see that the hydrogen production efficiency of 1847.9 μmol g^{-1} h^{-1} for the black-colored ZnO nanowires in our case is amongst the best values ever reported for the photocatalytic H_2 production of ZnO-based materials. Moreover, stability is always one of the major issues for photocatalysis. We note that for the photocatalytic hydrogen evolution study, the samples were tested for three hours, as shown in figures 4(c) and (d). The hydrogen evolution amount is linearly dependent on time in both cases during the three-hour investigation, which indicates that the ZnO/carbon sample is stable in the investigated time scale.

As for the enhancement mechanism of the hydrogen production for the carbon-incorporated sample, it is speculated that since the work function of carbon is lower than the Fermi level of ZnO, a heterojunction will form at the interface between ZnO and carbon, as illustrated in the inset of figure 5. When the samples are irradiated by UV–visible light, some of the photo-generated electrons in the ZnO will be transferred to carbon because of its lower energy level, while the holes in the ZnO will be sacrificed by the methanol solution. The recombination of photo-induced electrons and holes can be reduced in this way, thus the photocatalytic activity of the ZnO/carbon samples can be improved compared with that of the pristine ZnO. To confirm the carrier separation at the ZnO/carbon interface, the PL spectra of the pristine ZnO nanowires and carbon-incorporated nanowires under the excitation of the 325 nm line of a He–Cd laser were measured, as displayed in figure 5. For both samples, the spectra are dominated by an emission at around 375 nm, which can be attributed to the near-band-edge emission of ZnO [37], while the so-called deep level emission is almost negligible, which indicates that the incorporation of carbon has not induced deep levels within the bandgap of ZnO. Nevertheless,

one can find from the PL spectra that, under the same excitation conditions, the PL intensity of the pristine ZnO nanowires is much higher than that of the ZnO/carbon sample, which may result from the diffusion of some electrons from the conduction band of ZnO into the carbon. In addition, the introduced carbon can enhance the absorption of the visible light, which has been indicated in the absorption spectra shown in figure 4(a). That is the reason why the black carbon/ZnO sample shows better photocatalytic performance than the pristine one. The above data mean that, with the introduction of carbon into ZnO, more solar energy can be utilized, and the ZnO/carbon heterojunction helps the separation of electrons and holes, and thus the H_2 production capability has been improved.

4. Conclusions

In summary, carbon-incorporated ZnO nanowires have been synthesized via an MOCVD method, and the sample is black in color, which is different from the milky color of the common sample. The crystalline quality of the nanowires did not deteriorate much with the introduction of carbon into the ZnO. The absorption of the carbon-incorporated sample in the visible region has been increased greatly. The photocatalytic H_2 production activity of the carbon-incorporated sample is 2.5 times higher than that of the pristine sample, and amongst the best values ever reported for ZnO-based materials under simulated solar irradiation conditions. The enhancement mechanism can be attributed to the better separation of electrons and holes and better utilization of visible light. The results reported in this letter provide a common synthesis method of black-colored ZnO, thus may provide a route to high-performance ZnO photocatalysis.

Acknowledgments

This work was financially supported by the National Science Foundation for Distinguished Young Scholars of China (61425021), the Natural Science Foundation of China (11134009, 11374296, and 61177040).

References

[1] Zhu G, Liu Y, Xu H, Chen Y, Shen X and Xu Z 2012 Photochemical deposition of Ag nanocrystals on hierarchical ZnO microspheres and their enhanced gas-sensing properties *CrystEngComm* **14** 719–25

[2] Wu W, Zhang S, Xiao X, Zhou J, Ren F, Sun L and Jiang C 2012 Controllable synthesis, magnetic properties, and enhanced photocatalytic activity of spindlelike mesoporous alpha-$Fe_{(2)}O_{(3)}$/ZnO core–shell heterostructures *ACS Appl. Mater. Interfaces* **4** 3602–9

[3] Chen Y, Zeng D, Zhang K, Lu A, Wang L and Peng D L 2014 Au-ZnO hybrid nanoflowers, nanomultipods and nanopyramids: one-pot reaction synthesis and photocatalytic properties *Nanoscale* **6** 874–81

[4] Hu J J, Yuan H, Li P, Wang J, Liu Q K, Wang H, Wang Q L and Yuan X Y 2016 *Sci. China Chem.* **59** 277–81

[5] Oshima C, Nishiyama H, Chatterjee A, Uchida K, Sato K, Inoue Y, Hisatomi T and Domen K 2015 Photocatalytic activity of ZnO/$GaP_{1-x}N_x$ for water splitting *J. Mater. Chem.* A **3** 18083–9

[6] Hong Y, Tian C G, Jiang B J, Wu A P, Zhang Q, Tian G H and Fu H G 2013 Facile synthesis of sheet-like ZnO assembly composed of small ZnO particles for highly efficient photocatalysis *J. Mater. Chem.* A **1** 5700–8

[7] Gao P, Liu Z Y and Sun D D 2013 The synergetic effect of sulfonated graphene and silver as co-catalysts for highly efficient photocatalytic hydrogen production of ZnO nanorods *J. Mater. Chem.* A **1** 14262–9

[8] Cao Y Q, Chen J, Zhou H, Zhu L, Li X, Cao Z Y, Wu D and Li A D 2015 Photocatalytic activity and photocorrosion of atomic layer deposited ZnO ultrathin films for the degradation of methylene blue *Nanotechnology* **26** 024002

[9] Zhou X, Li Y, Peng T, Xie W and Zhao X 2009 Synthesis, characterization and its visible-light-induced photocatalytic property of carbon doped ZnO *Mater. Lett.* **63** 1747–9

[10] Xu Y, Xu H, Li H, Xia J, Liu C and Liu L 2011 Enhanced photocatalytic activity of new photocatalyst Ag/AgCl/ZnO *J. Alloys. Compd.* **509** 3286–92

[11] Mu J, Shao C, Guo Z, Zhang Z, Zhang M, Zhang P, Chen B and Liu Y 2011 High photocatalytic activity of ZnO-carbon nanofiber heteroarchitectures *ACS Appl. Mater. Interfaces* **3** 590–6

[12] Lv Y, Yu L, Huang H, Feng Y, Chen D and Xie X 2012 Application of the soluble salt-assisted route to scalable synthesis of ZnO nanopowder with repeated photocatalytic activity *Nanotechnology* **23** 065402

[13] Lu W, Liu G, Gao S, Xing S and Wang J 2008 Tyrosine-assisted preparation of Ag/ZnO nanocomposites with enhanced photocatalytic performance and synergistic antibacterial activities *Nanotechnology* **19** 445711

[14] Lin L, Yang Y, Men L, Wang X, He D, Chai Y, Zhao B, Ghoshroy S and Tang Q 2013 A highly efficient TiO_2@ZnO n-p-n heterojunction nanorod photocatalyst *Nanoscale* **5** 588–93

[15] Han Z, Ren L, Cui Z, Chen C, Pan H and Chen J 2012 Ag/ZnO flower heterostructures as a visible-light driven photocatalyst via surface plasmon resonance *Appl. Catal.* B **126** 298–305

[16] Guo Y, Wang H, He C, Qiu L and Cao X 2009 Uniform carbon-coated ZnO nanorods: microwave-assisted preparation, cytotoxicity, and photocatalytic activity *Langmuir* **25** 4678–84

[17] Faisal M, Ibrahim A A, Harraz F A, Bouzid H, Al-Assiri M S and Ismail A A 2015 SnO_2 doped ZnO nanostructures for highly efficient photocatalyst *J. Mol. Catal.* A **397** 19–25

[18] Li S S, Chang C P, Lin C C, Lin Y Y, Chang C H, Yang J R, Chu M W and Chen C W 2011 Interplay of three-dimensional morphologies and photocarrier dynamics of polymer/TiO_2 bulk heterojunction solar cells *J. Am. Chem. Soc.* **133** 11614–20

[19] Zhang X, Qin J, Hao R, Wang L, Shen X, Yu R, Limpanart S, Ma M and Liu R 2015 Carbon-doped ZnO nanostructures: facile synthesis and visible light photocatalytic applications *J. Phys. Chem.* C **119** 20544–54

[20] Zhang K Z, Lin B Z, Chen Y L, Xu B H, Pian X T, Kuang J D and Li B 2011 Fe-doped and ZnO-pillared titanates as visible-light-driven photocatalysts *J. Colloid Interface Sci.* **358** 360–8

[21] Wu C, Shen L, Zhang Y-C and Huang Q 2011 Solvothermal synthesis of Cr-doped ZnO nanowires with visible light-driven photocatalytic activity *Mater. Lett.* **65** 1794–6

[22] Muthulingam S, Bae K B, Khan R, Lee I-H and Uthirakumar P 2015 Improved daylight-induced photocatalytic performance and suppressed photocorrosion of N-doped ZnO decorated with carbon quantum dots *RSC Adv.* **5** 46247–51
[23] Lin Y G, Hsu Y K, Chen Y C, Chen L C, Chen S Y and Chen K H 2012 Visible-light-driven photocatalytic carbon-doped porous ZnO nanoarchitectures for solar water-splitting *Nanoscale* **4** 6515–9
[24] Karunakaran C, Rajeswari V and Gomathisankar P 2011 Combustion synthesis of ZnO and Ag-doped ZnO and their bactericidal and photocatalytic activities *Superlattices Microstruct.* **50** 234–41
[25] Jia X, Fan H, Afzaal M, Wu X and O'Brien P 2011 Solid state synthesis of tin-doped ZnO at room temperature: characterization and its enhanced gas sensing and photocatalytic properties *J. Hazard Mater.* **193** 194–9
[26] Haibo O, Feng H J, Cuiyan L, Liyun C and Jie F 2013 Synthesis of carbon doped ZnO with a porous structure and its solar-light photocatalytic properties *Mater. Lett.* **111** 217–20
[27] Cho S, Jang J-W, Lee J S and Lee K-H 2010 Carbon-doped ZnO nanostructures synthesized using vitamin C for visible light photocatalysis *CrystEngComm* **12** 3929
[28] Xia T and Chen X 2013 Revealing the structural properties of hydrogenated black TiO_2 nanocrystals *J. Mater. Chem.* A **1** 2983
[29] Chen X, Liu L, Yu P Y and Mao S S 2011 Increasing solar absorption for photocatalysis with black hydrogenated titanium dioxide nanocrystals *Science* **331** 10
[30] Chen X *et al* 2013 Properties of disorder-engineered black titanium dioxide nanoparticles through hydrogenation *Sci. Rep.* **3** 1510
[31] Xia T, Wallenmeyer P, Anderson A, Murowchick J, Liu L and Chen X B 2014 Hydrogenated black ZnO nanoparticles with enhanced photocatalytic performance *RSC Adv.* **4** 41654–8
[32] Chang C-J, Huang K-L, Chen J-K, Chu K-W and Hsu M-H 2015 Improved photocatalytic hydrogen production of ZnO/ZnS based photocatalysts by Ce doping *J. Taiwan Inst. Chem. Eng.* **55** 82–9
[33] Hong E and Kim J H 2014 Oxide content optimized ZnS–ZnO heterostructures via facile thermal treatment process for enhanced photocatalytic hydrogen production *Int. J. Hydrogen Energy* **39** 9985–93
[34] Yu Z B, Xie Y P, Liu G, Lu G Q, Ma X L and Cheng H-M 2013 Self-assembled CdS/Au/ZnO heterostructure induced by surface polar charges for efficient photocatalytic hydrogen evolution *J. Mater. Chem.* A **1** 2773
[35] Yuan Y J, Wang F, Hu B, Lu H W, Yu Z T and Zou Z G 2015 Significant enhancement in photocatalytic hydrogen evolution from water using a MoS_2 nanosheet-coated ZnO heterostructure photocatalyst *Dalton Trans.* **44** 10997–1003
[36] Lu X H, Wang G M, Xie S L, Shi J Y, Li W, Tong Y X and Li Y 2012 Efficient photocatalytic hydrogen evolution over hydrogenated ZnO nanorod arrays *Chem. Commun.* 7717–9
[37] Fan H J, Bertram F, Dadgar A, Christen J, Krost A and Zacharias M 2004 Self-assembly of ZnO nanowires and the spatial resolved characterization of their luminescence *Nanotechnology* **15** 1401–4